Hydration and anomalous solubility of the Bell-Lavis model as solvent

Marcia M. Szortyka,[1,*] Carlos E. Fiore,[2,†] Marcia C. Barbosa,[3,‡] and Vera B. Henriques[4,§]

[1]*Departamento de Física, Universidade Federal de Santa Catarina, Caixa Postal 476, 88010-970 Florianópolis, Santa Catarina, Brazil*

[2]*Departamento de Física, Universidade Federal do Paraná, Caixa Postal 19044, 81531 Curitiba, Paraná, Brazil*

[3]*Instituto de Física, Universidade Federal do Rio Grande do Sul, Caixa Postal 15051, 91501-970 Porto Alegre, Rio Grande do Sul, Brazil*

[4]*Instituto de Física, Universidade de São Paulo, Caixa Postal 66318, 05315970 São Paulo, São Paulo, Brazil*

(Received 8 July 2012; published 12 September 2012)

We address the investigation of the solvation properties of the minimal orientational model for water originally proposed by [Bell and Lavis, J. Phys. A **3**, 568 (1970)]. The model presents two liquid phases separated by a critical line. The difference between the two phases is the presence of structure in the liquid of lower density, described through the orientational order of particles. We have considered the effect of a small concentration of inert solute on the solvent thermodynamic phases. Solute stabilizes the structure of solvent by the organization of solvent particles around solute particles at low temperatures. Thus, even at very high densities, the solution presents clusters of structured water particles surrounding solute inert particles, in a region in which pure solvent would be free of structure. Solute intercalates with solvent, a feature which has been suggested by experimental and atomistic simulation data. Examination of solute solubility has yielded a minimum in that property, which may be associated with the minimum found for noble gases. We have obtained a line of minimum solubility (TmS) across the phase diagram, accompanying the line of maximum density. This coincidence is easily explained for noninteracting solute and it is in agreement with earlier results in the literature. We give a simple argument which suggests that interacting solute would dislocate TmS to higher temperatures.

DOI: 10.1103/PhysRevE.86.031503 PACS number(s): 64.70.Ja, 64.70.F−, 78.55.Bq

I. INTRODUCTION

Biological molecules are functional only if organized spatially in very specific arrangements. This is the case for phospholipids in membranes, proteins soluble in water, membrane proteins, cholesterol, or lipoproteins. One of the main ingredients behind spatial organization is solubility: globular proteins maintain their polar moieties on the exterior, in contact with water, while membrane proteins must turn their polar parts inwards, avoiding contact with the hydrophobic bilayer core.

Solubility depends on chemical structure, but varies with temperature. For simple substances, the behavior of solubility with temperature is dependent on miscibility, which describes the relative affinities of the molecules in solution [1]. The reasoning is simple. If we consider the solution phase in equilibrium with the gas phase, two situations exist. Consider X to be the solute in solvent Y. If Y and X "prefer" mixing, which means that the energy of a YX pair is lower than the average energy of YY and XX pairs, for the solution energy to increase as the temperature goes up, X must necessarily leave the solution, thus making solubility decrease. On the contrary, if Y and X prefer to phase separate, at low temperatures X will go preferentially to the gas phase. However, as the temperature goes up, the solution energy increases while X dissolves in Y, making the solubility go up.

Solubility in water is different. Noble gases, for instance, present a temperature of minimum solubility in water at atmospheric pressure [2]. Water presents in numerous thermodynamic and dynamic anomalies, and the minimum in solubility is one of them. The origin of the anomalies has been investigated theoretically both for statistical and atomistic models. However, a simple complete picture has not yet emerged.

The presence of a hydrogen-bond network was suggested by Bernal and Fowler [3] in order to explain the large mobility of H^+ and OH^- ions: the latter could only be explained if protons would jump between neighboring properly oriented molecules in liquid water. The idea of an extensive H bond network and a corresponding water structure has been studied with x-rays for many years, and the presence of the network has been confirmed by more recent neutron scattering experiments, which point to an even more stable structure than previously believed [4]. Hydrogen bonds are considered a key feature in biochemistry [5].

The presence of an H-bond network could qualitatively explain the well-known maximum in density. The disordering of bonds allows density to increase with temperature since the entropy of the bonds increases while translational entropy decreases, maintaining the necessary positive entropy balance. The two entropic effects compete up to a temperature at which translational entropy wins over orientational entropy, lowering density, as in more "usual" substances.

The dynamically connected molecules would also be able to explain the minimum in solubility. The contraction of the solvent, driven by decreasing orientational entropy, excludes the solute. Thus a decreasing solubility is a consequence of an increasing density of the solvent. In this case, the energy of the interactions enters only either to favor the decreasing solubility or to compete with it.

The study of statistical models capable of displaying properties typical of water has led, in the last years, to two basic models: (i) orientational models [6–13], which reflect the H-bonding property of water, and (ii) two-scale isotropic models, inspired by the low-temperature low-density property of water.

*szortyka@gmail.com
†fiore@fisica.ufpr.br
‡marcia.barbosa@ufrgs.br
§vera@if.usp.br

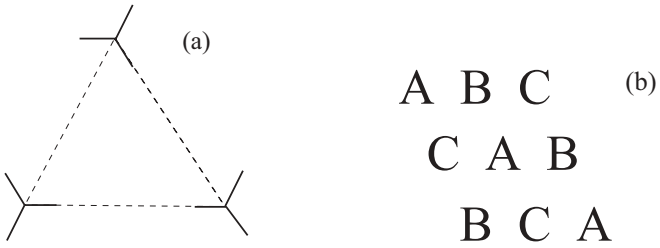

FIG. 1. (a) The arm variables in the triangular lattice. Pairs of particles of opposite orientation hydrogen bond. Pairs of the same orientation do not bond. (b) The three sublattices: A, B, and C.

Both models present several of the anomalous features of water [14–27]. However, the second kind of model does not involve specific orientation of low-energy pairs of particles: pair energy is controlled by distance, not by orientation. This poses a question of the relevance of the microscopic bonding in relation to the macroscopic properties.

In this study we propose to contribute to further investigation of the relation between the solvent structure and solubility. The role of cavity formation in the explanation of hydrophobic interactions has been recognized by Pratt and Chandler [28–30]. They have examined the difference between cavity formation in associating and simple liquids [29,30]. A thorough investigation of noble gas solubility has been undertaken by Guillot and Guissani [31] from the point of view of atomistic models. Our approach is that of a minimal statistical model. We consider a two-dimensional lattice model proposed originally by Bell and Lavis [7] and shown by us [25,27] to exhibit many anomalous properties despite the absence of liquid polymorphism. In this study we add noninteracting solute particles which occupy a single lattice site in order to investigate the effect of solute on solvent properties as well as the effect of solute solubility.

The paper is organized as follows. In Sec. II the model without and with solute is introduced, simulation details are presented in Sec. III, the phase diagram of the system with solute is shown in Sec. IV, the solubility is analyzed in Sec. V, and conclusions are given in Sec. VI.

II. THE BELL-LAVIS MODEL AS SOLVENT

The Bell-Lavis (BL) model is defined on a triangular lattice where each site may be empty ($\sigma_i = 0$) or occupied ($\sigma_i = 1$) by an anisotropic water molecule [7]. Each particle has two orientational states that may be described in terms of six "arm" variables, τ_i^{ij}, with $\tau_i^{ij} = 1$ for the bonding state and $\tau_i^{ij} = 0$ for the inert arm state as illustrated in Fig. 1(a). A pair of adjacent molecules interacts via van der Waals with energy $\epsilon_{\rm vdw}$, as well as through "hydrogen bonds" of energy $\epsilon_{\rm hb}$, whenever bonding arms point to each other ($\tau_i^{ij}\tau_j^{ji} = 1$). The model is defined by the following effective Hamiltonian in the grand-canonical ensemble:

$$\mathcal{H} = -\sum_{\langle i,j\rangle} \sigma_i\,\sigma_j\left(\epsilon_{\rm hb}\,\tau_i^{ij}\,\tau_j^{ji} + \epsilon_{\rm vdw}\right) - \mu\sum_i \sigma_i, \qquad (1)$$

where $\epsilon_{\rm vdw}$ and $\epsilon_{\rm hb}$ are the van der Waals and hydrogen bond interaction energies, respectively, and μ is the chemical potential.

The model phase diagram features depend on the ratio $\zeta = \epsilon_{\rm vdw}/\epsilon_{\rm hb}$ (see insets of Fig. 2 that illustrate the reduced chemical potential versus the reduced temperature for two cases of bond strength: weaker, $\zeta = 1/4$, and stronger, $\zeta = 1/10$). For $\zeta < 1/3$, besides the gas phase, the model exhibits two liquid phases with different structures. At $\bar{T} = 0$, coexistence between a gas and a structured liquid of low density (SL) and coexistence between the structured low-density liquid and the nonstructured high-density liquid are present [32]. However, for finite temperatures, the transition between the two liquids

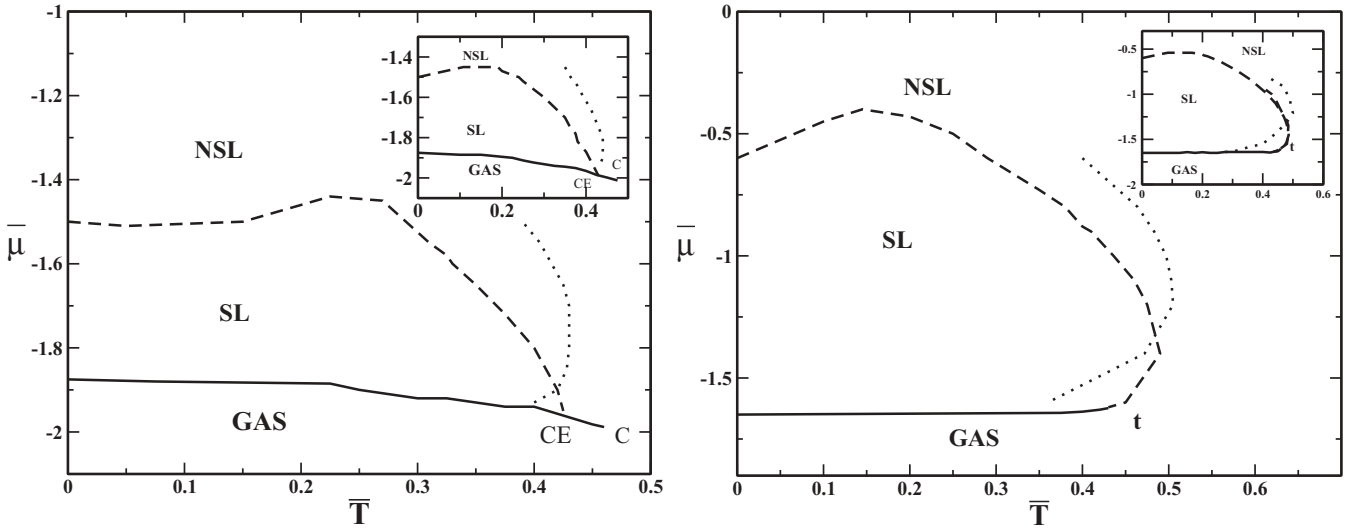

FIG. 2. Solvent chemical potential $\bar{\mu}$ vs reduced temperature $\bar{T}$ phase diagram for model solution at solute concentration 2% and (a) $\zeta = 1/4$ and (b) $\zeta = 1/10$. Solid, dashed, and dotted lines correspond to first-order phase transitions, second-order phase transitions, and the TMD, respectively. The symbols C, CE, and t denote critical, critical-ending, and tricritical points, respectively. The insets display the corresponding phase diagram for pure solvent for comparison.

becomes critical, as shown from detailed systematic analysis of simulational data [25]. The two liquid phases do not coexist and the density varies continuously at the phase transition as shown by susceptibility measurements on sublattice density fluctuations [27]. In order to stress the absence of a density gap we denominate the two liquid phases as structured (SL) and nonstructured liquid (NSL), instead of adopting the usual low-density liquid (LDL) and high-density liquid (HDL) nomenclature. The difference between the two liquid phases lies in the orientational and translational order of the bonding particles. The SL phase presents a large population of particles in two of the three sublattices [see Fig. 1(b)] associated with a large bonding network, whereas in the NSL the density is close to 1 and orientational order is lost. The increase in the temperature and the increase in the chemical potential favor the NSL phase. In the case of the stronger hydrogen bonds ($\zeta = 1/10$) the SL is favored and the transition occurs for higher chemical potentials.

A line of temperatures of maximum density (TMD) lies near the critical line separating the two liquid phases. Its pressure and temperature location is not very sensitive to the strength of the hydrogen bonds; in the $\zeta = 1/10$ case at low chemical potentials the TMD line is located in the SL phase while for high chemical potentials it is located at the critical line. In this work we have added inert apolar solutes to the BL model. The new particles occupy empty sites and thus interact only via excluded volume with the BL solvent particles. Our purpose is the investigation of the effect of the apolar solute upon the TMD and the regions of stability of the low- and high-density phases. Here we address the following questions. What would be the effect of adding solute to the structured liquid? Under what circumstances does phase separation occur? Is there a solubility minimum? In the latter case, can we establish a relation between the density and the solubility anomalies?

III. MONTE CARLO SIMULATIONS

We have investigated the properties of our model solution through Monte Carlo simulations, in a mixed ensemble, of fixed chemical potential for solvent and constant density for the apolar solute, under periodic boundary conditions.

The model solvent microscopic configurations were generated through randomly selected exclusion, insertion, or rotation of water particles, whereas solute movements were based on solvent-solute and hole-solute exchanges. Acceptance rates are those of the usual Metropolis algorithm: transitions between two configurations are accepted according to the Metropolis prescription $\min\{1, \exp(-\beta\Delta\mathcal{H})\}$, where $\Delta\mathcal{H}$ is the effective energy difference between the two states. Our simulations were carried out for lattice sizes ranging from $L = 30$ to $L = 60$. Results shown here are for $L = 30$. All the thermodynamic quantities are expressed in reduced units of ϵ_{hb} and lattice distance.

IV. SOLVENT PHASE DIAGRAM IN THE PRESENCE OF INERT SOLUTE

We have investigated how the chemical potential versus temperature phase diagram changes by the addition of an inert solute. We study this employing two solute concentrations, 2% and 10%.

The reduced chemical potential versus reduced temperature phase diagrams for both weak and strong bonds, $\zeta = 1/4$ and $\zeta = 1/10$, and a concentration of 2% of solute are shown in Fig. 2. At this small concentration of solute, the phase diagram suffers small quantitative changes: the structure's SL phase extends to slightly higher chemical potential, while, in the case of weaker bonds, $\zeta = 1/4$, the TMD line moves into the SL phase at low temperature. Thus solute stabilizes the SL to higher chemical potential, which suggests a reinforcement of hydrogen bonding. It also brings down the temperature of maximum density in the case of weaker bonds, resulting in TMD behavior similar to that of the case of stronger bonds—again, solute seems to "strengthen" bonds.

Figure 3 illustrates features of the solution structure in the case of strong bonds, $\zeta = 1/10$ and a concentration of 2% of solute. The triangular lattice is subdivided into three sublattices as illustrated in Fig. 1(b). The orientation and density of solvent particles as well as the density of solute are computed on each sublattice.

The first set of data in Figs. 3(a)–3(c) illustrate the orientation of the solvent molecules, the density of solvent, and the density of the solute versus temperature for $\bar{\mu} = -1.6$. Each sublattice is defined by the color and the line style. The graphs show the transition between the NSL and the SL phase by decreasing the temperature. It can be seen that in the SL phase ($\bar{\mu} = -1.6$) solvent occupies mainly two of the sublattice (with $\rho_{\mathrm{solvent}} \approx 1$ at $\bar{T} = 0.3$), with complementary orientations ($m = +1$ and $m = -1$), indicating strong bonding. Both quantities vary abruptly at the transition to the NSL phase, around $\bar{T} = 0.45$, with homogeneous occupation and orientation of the molecules on the three sublattices. As for solute, at the lower temperature, $\bar{T} = 0.3$, occupation of the empty sublattice is preferential ($\rho_{\mathrm{solute}} \approx 2\%$), while the other sublattices are nearly empty. As solvent disorders on the sublattice, around $\bar{T} = 0.45$, solute densities vary continuously towards homogeneous occupations of the three sublattices.

Figures 3(e) and 3(f) illustrate the same data as before but for the reduced chemical potential $\bar{\mu} = -0.4$. In this case, no transition is observed. The system is in the NSL phase even at low temperature, and sublattice solvent orientation and solute density vary continuously towards homogeneous distribution on the sublattice. Solvent density still carries the signature of the ordered phase, transitioning smoothly to disorder in a sigmoidal fashion.

Figure 4 displays the reduced chemical potential versus reduced temperature phase diagrams for 10% concentration of the solute, for both values of hydrogen bond strength $\zeta = 1/4$ (left) and $\zeta = 1/10$ (right). In this case substantial change in the phase diagrams can be seen. The low-temperature SL to NSL phase transition seen as one increases chemical potential for pure solvent is destroyed by the presence of solute. Instead, the transition may be reached only from temperature variations, and the SL phase extends to very high chemical potentials. The TMD line moves nearer to the critical SL-NSL line and crosses into the SL phase.

In Fig. 5 we investigate the solvent orientation and density as well as the density of solute in each sublattice in different

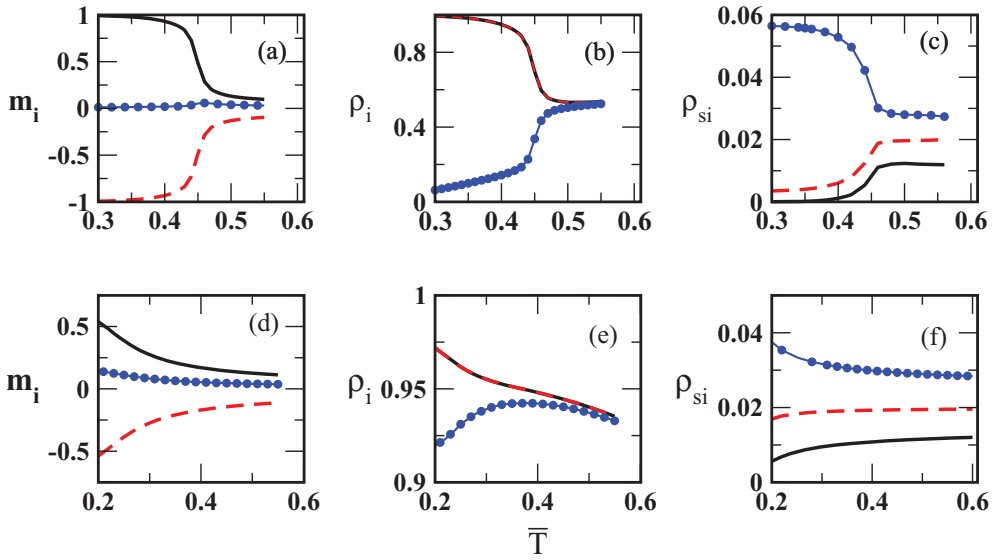

FIG. 3. (Color online) Sublattice distributions for solvent and solute properties for 2% solute concentration and $\zeta = 1/10$. From right to left, we have solvent particle orientation m_i, solvent particle density ρ_i, and solute density ρ_{si} versus reduced temperature $\bar{T}$. The top graphs are for the lower reduced chemical potential $\bar{\mu} = -1.6$, and the bottom graphs are for the higher reduced chemical potential $\bar{\mu} = -0.4$. Colors and line style define each sublattice.

regions of the phase diagram at 10% solute concentration for bond strength $\zeta = 1/10$. For both low, $\bar{\mu} = -1.3$, and high, $\bar{\mu} = 4.0$, reduced chemical potential, solute orders together with solvent at low temperatures. As can be seen, from the color and line style of each sublattice, solute goes into the empty lattice while solvent particles orient properly on two sublattices in order to connect through bonds.

For both reduced chemical potentials an abrupt variation of the solvent density, of the solute density, and of the solvent orientation occur simultaneously, near $\bar{T} = 0.45$ for $\bar{\mu} = -1.3$ and near $\bar{T} = 0.3$ for $\bar{\mu} = 4.0$ at the SL-NSL transition line.

However, despite the qualitative similar behavior there are quantitative important differences between the two regions of chemical potential. For the lower chemical potential, $\bar{\mu} = -1.3$, solvent behavior is similar to that of pure solvent. The orientationally ordered solvent particles occupy mainly two of the sublattices, while the third sublattice remains nearly free of solvent. At $\bar{T} = 0.3$ nearly 60% of that sublattice stands vacant, while solute particles occupy 30% of the sites, leaving the other two sublattice free of solute.

At high chemical potential, $\bar{\mu} = 4.0$, while solute maintains the 30% occupancy of one of the sublattices at low temperature, the solvent particles fill up the rest of the sublattice sites, reaching 70% occupancy of that sublattice.

The new behavior induced by the presence of solute is better understood by comparing Figs. 3(e) and 5(e). Differently from

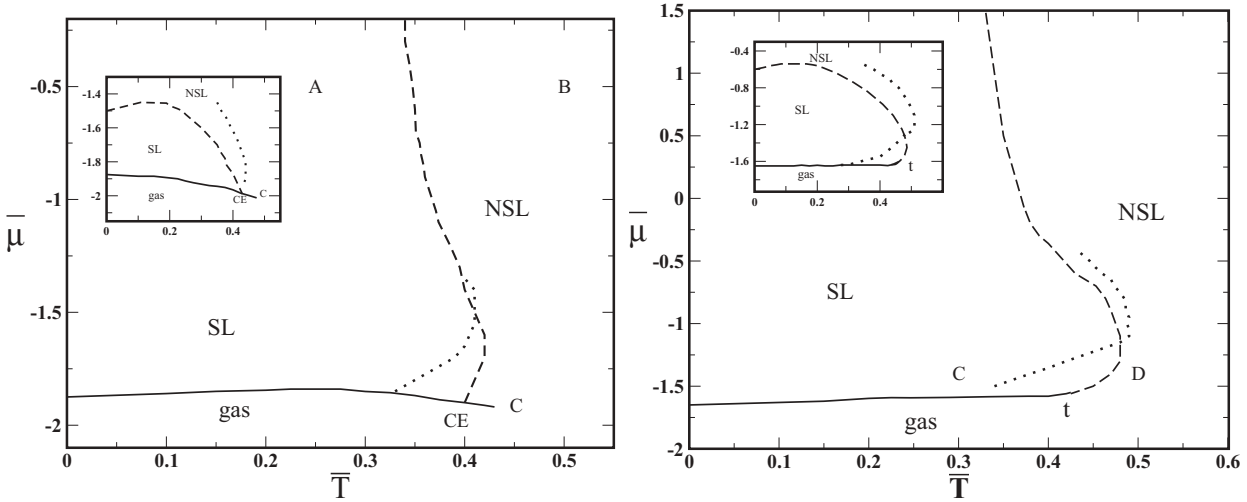

FIG. 4. Solvent reduced chemical potential $\bar{\mu}$ versus reduced temperature $\bar{T}$ phase diagram for model solution at solute concentration 10% for (a) $\zeta = 1/4$ and (b) $\zeta = 1/10$. Solid, dashed, and dotted lines correspond to first-order phase transitions, second-order phase transitions, and the TMD, respectively. The symbols CE, C, and t denote critical-ending, critical, and tricritical points, respectively. The insets display the corresponding phase diagrams for pure solvents for comparison.

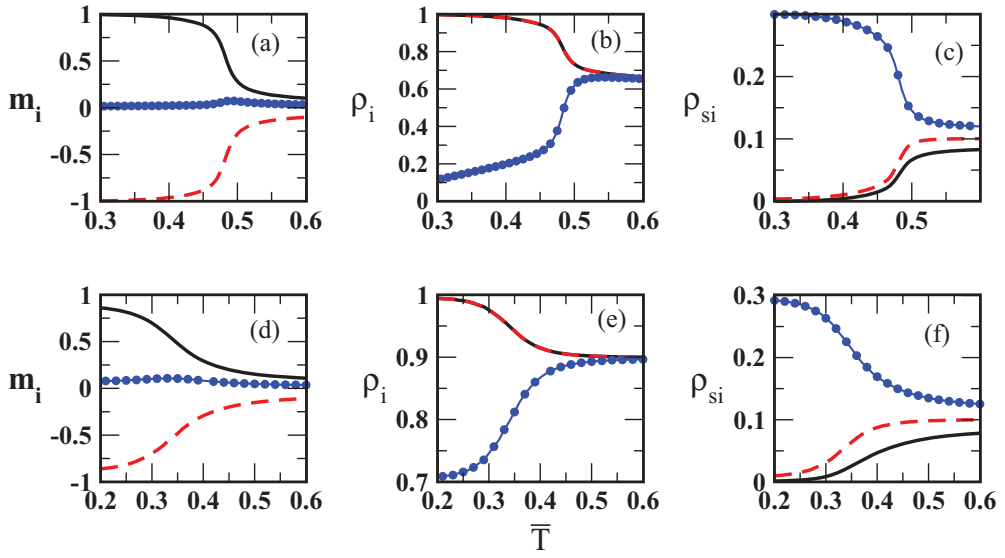

FIG. 5. (Color online) Solution structure in the new phase. Sublattice solvent particle orientation m_i, solvent density ρ_i, and solute density ρ_{si} vs temperature for different chemical potentials for 10% of solute concentration and $\zeta = 1/10$. The top and bottom graphs correspond to solvent chemical potentials $\mu = -1.30$ and $\mu = 4.0$.

the 2% solute concentration, for the 10% concentration case the filling up of the lattice yields only partial rupture of hydrogen bonding. Maintenance of the hydrogen-bond network at such high density seems to be a result of the structuring effect of solute.

Inspection of typical configurations in different regions of the phase diagrams are quite useful at this point. Figures 6 and 7 display snapshots of the model system at different points (indicated by letters in Fig. 4) in the reduced chemical potential versus reduced temperature phase diagrams with a solute concentration of 10%.

For $\zeta = 1/4$ (Fig. 6), at $\bar{\mu} = -0.50$ and $\bar{T} = 0.25$ (inside SL phase, point A in Fig. 4), the lattice is filled up, but patches of structured liquid can be seen with solute localizing only in sites which contribute to organizing the hydrogen-bond network. As the SL-NSL line is crossed and for $\bar{T} = 0.50$ (point B in Fig. 4), a few isolated solute particles are surrounded by water particle structure, while most solute particles are clustered in vacant regions.

For $\zeta = 1/10$ (Fig. 7), at $\bar{\mu} = -1.40$ and $\bar{T} = 0.30 < \bar{T}_{\mathrm{TMD}}$ (point C in Fig. 4), a fully bonded network of solvent particles is accompanied by solute particles located in the empty sublattice. This gives rise to apparently linear aggregates intercalated by solvent. At a temperature higher than the TMD, $\bar{T} = 0.50$ (point D in Fig. 4), some bonding of the solvent particles in hexagons are still seen, with intercalated solute. However, the system is much less dense, and solute particles also localize in large vacant regions.

V. MODEL SOLUBILITY

The Ostwald solubility Σ is defined as the ratio between solute densities ρ_X in the two coexisting phases:

$$\Sigma = \frac{\rho_X^{\mathrm{I}}}{\rho_X^{\mathrm{II}}}.$$

The two coexisting phases, I and II, might be either a gas phase II that coexists with a homogeneous liquid phase I [31] or two liquid phases, I and II, of different relative densities, the first poor in solute X and the other rich in X [33].

In the case of liquid-liquid phase separation, the form of the temperature-density coexistence curve, at fixed pressure, is indicative of solubility behavior. If the density gap decreases as the temperature is increased, the solubility increases with

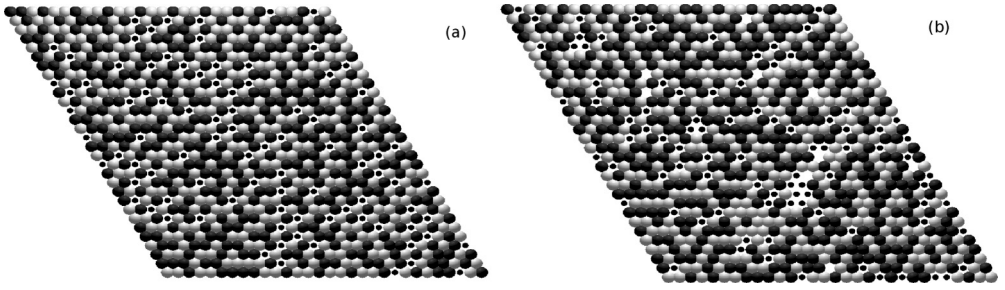

FIG. 6. Snapshots of model system for a concentration of 10% and $\zeta = 1/4$ at high chemical potential, $\bar{\mu} = -0.5$, at (a) point A ($\bar{T} = 0.25$, left) and (b) point B ($\bar{T} = 0.5$, right) in Fig. 4. Black and gray circles represent the two possible orientations of solvent particles [see Fig 1(a)]; black dots represent solute particles.

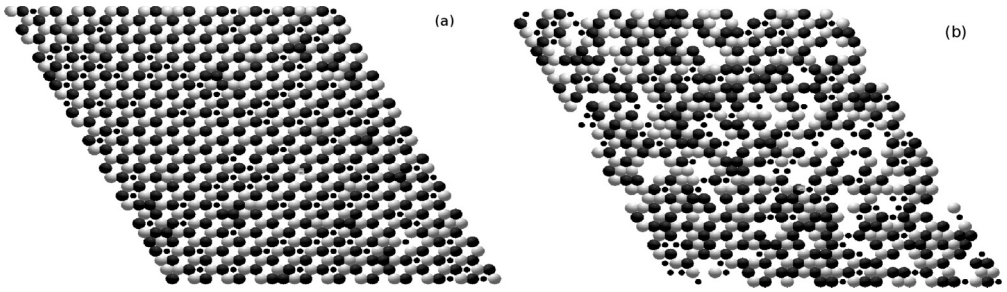

FIG. 7. Snapshots of model system for a concentration of 10% and $\zeta = 1/10$ at low chemical potential, $\bar{\mu} = -1.4$, at (a) point C ($\bar{T} = 0.3$, left) and (b) point D ($\bar{T} = 0.5$, right) in Fig. 4. Black and gray circles represent the two possible orientations of solvent particles [see Fig 1(a)]; black dots represent solute particles.

the temperature. However, for reentrant coexistence curves, for which the density gap increases as the temperature is increased, solubility decreases as the temperature is raised.

On the other hand, minimal statistical models show that for dense lattice gas solutions with isotropic van der Waals-like interactions solubility behaves univocally with temperature. Coexistence densities between an ideal gas mixture and a lattice dense solution, for substances Y and X, are obtained from the equality of the corresponding chemical potentials. Consider interaction constants w_{YY}, w_{XX}, and w_{YX} between pairs YY, XX, and YX. For solute X in the gas phase given by the dimensionless solute X density ρ_X^{gas}, we might write

$$\mu_X^{\text{gas}} = k_B T \ln \rho_X^{\text{gas}}, \tag{3}$$

whereas for solute X in the dense lattice solution, we have

$$\mu_X^{\text{solution}} = \frac{w_{XX}}{2} - \frac{w}{2}(1 - x_X)^2 + k_B T \ln x_X^{\text{solution}}, \tag{4}$$

where $w = w_{YY} + w_{XX} - 2w_{YX}$ and x_X is the solution concentration given in mole fraction. Equating Eq. (3) to Eq. (4) yields

$$\frac{x_X^{\text{solution}}}{\rho_X^{\text{gas}}} = e^{-\frac{\beta w_{XX}}{2}} e^{\frac{\beta w}{2}(1-x_X^{\text{solution}})^2}. \tag{5}$$

A slightly different definition of solubility, proportional to the inverse of Henry's constant, is given by

$$\Sigma' = \frac{x_X^{\text{solution}}}{\rho_X^{\text{gas}} / \rho_X^0}, \tag{6}$$

where ρ_X^0 is gas density for pure liquid X. Comparing Eq. (5) with Eq. (6) gives

$$\Sigma' = e^{\frac{\beta w}{2}(1-x_X^{\text{solution}})^2}. \tag{7}$$

Thus for poorly miscible solutions, with $w < 0$, which phase separate at low temperatures, solubility increases with temperature, since $d\Sigma'/dT \propto -w$. On the other hand, if the two liquids are miscible, when $w > 0$, solubility decreases as the temperature is raised. In either case, solubility displays monotonic behavior with temperature.

The solubility behavior of the dense lattice model is the result of a competition between entropy of mixture and an isotropic interaction potential. The model misses the role of density, an essential feature of water.

How does the introduction of asymmetry into the interaction potential, accompanied by orientational entropy, change this picture? In order to answer to this question we have measured the solubility of our model inert solute as a function of temperature for different fixed chemical potentials of solvent by assuming the coexistence of a gas (phase Y) and a homogeneous solution phase (X). The gas phase was assumed to be ideal, thus

$$\mu_X^{\text{gas}} = -k_B T \ln \rho_X^{\text{gas}}. \tag{8}$$

For the solution phase, the chemical potential of the solute was calculated from simulation data through Widom's insertion method [34]. In our semigrand canonical ensemble the semigrand potential $\psi = \psi(T, V, N_X, \mu)$ depends on T, V, N_X, and the solvent chemical potential μ. In the thermodynamic limit, the solute chemical potential $\mu_X^{\text{solution}} = -(\frac{\partial \psi}{\partial N_X})$ can be approximated by the difference $\psi(T, V, N_X + 1, \mu) - \psi(T, V, N_X, \mu)$ and we have

$$\mu_X^{\text{solution}} = -k_B T \ln \frac{\Xi(T, V, \mu, N_{X+1})}{\Xi(T, V, \mu, N_X)}, \tag{9}$$

which relates average values in two different ensembles of N_X and N_{X+1} particles. However, the numerator can be interpreted in terms of an average in the ensemble of N_X solute particles. Thus we have

$$\mu_X^{\text{solution}} = -k_B T \ln \left(\frac{1}{\langle \rho_X^{\text{solution}} \rangle} \right) \langle e^{-\beta \Delta u} \rangle_{T, V, N_X, \mu}, \tag{10}$$

where Δu is the additional energy due to insertion of solute molecules to a system of solute concentration $\rho_X^{\text{solution}} = N_X / V$. Finally, by equating μ_X^{solution} and μ_X^{gas}, we obtain the following for the solubility:

$$\Sigma = \frac{\rho_X^{\text{solution}}}{\rho_X^{\text{gas}}} = \langle e^{-\beta \Delta u} \rangle_{T, V, N_X, \mu}. \tag{11}$$

In Fig. 8 we display our data for solubility Σ versus temperature for bond strength $\zeta = 1/10$. As can be seen, a minimum is present for different chemical potentials of solvent.

The temperature of minimum solubility (TmS) coincides entirely with the TMD in the $\bar{\mu}$ vs $\bar{T}$ plane. This is to be expected for inert solutes. Inspection of Eq. (11) for inert solutes yields $\exp\{-\beta \Delta u\} = 1$ for insertion into empty sites and yields 0 otherwise. Thus solubility can be directly related to the overall liquid density $(N_X + N^{\text{solvent}})/V$. Thus

$$\Sigma = \langle e^{-\beta \Delta u} \rangle_{T, V, N_X, \mu} = 1 - \rho^{\text{solvent}} - \rho_X^{\text{solute}}, \tag{12}$$

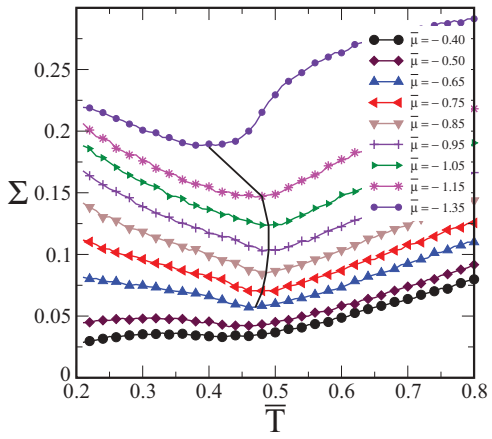

FIG. 8. (Color online) Ostwald coefficient Σ versus $\overline{T}$ for different $\overline{\mu}$ for $\zeta = 1/10$ and 10%. The black line corresponds to the temperature for which the density presents a maximum.

and for fixed solute density

$$\frac{d\Sigma}{dT} = -\frac{d\rho^{\text{solvent}}}{dT}, \tag{13}$$

and therefore the TMD is accompanied by the TmS. Is the coincidence between TmS and TMD restricted to inert solutes?

It is tempting to extend our analysis of Eq. (11) to interacting solutes. A first simplest approach to the question would be to investigate the energetic effect on solubility through the following approximation

$$\Sigma = \langle e^{-\beta \Delta u} \rangle_{T,V,N_X,\mu} \approx \left(1 - \rho^{\text{solvent}} - \rho_X^{\text{solute}}\right) e^{-\beta \langle \Delta u \rangle}, \tag{14}$$

thus

$$\frac{d\Sigma}{dT} \approx \left[-\frac{d\rho^{\text{solvent}}}{dT} + \left(1 - \rho^{\text{solvent}} - \rho_X^{\text{solute}}\right) \times \left(\frac{\langle \Delta u \rangle}{k_B T^2} - \beta \frac{d\langle \Delta u \rangle}{dT} \right) \right] e^{-\beta \langle \Delta u \rangle}. \tag{15}$$

Since $\langle \Delta u \rangle$ is necessarily negative and $\frac{d\langle \Delta u \rangle}{dT}$ is necessarily positive, this result implies that the minimum in solubility should occur at a temperature higher than TMD. This is in accordance with data on the solubility of gases.

VI. CONCLUSIONS

In this paper we have considered the investigation of the thermodynamic phases and of solubility of the BL water model in the presence of a small concentration of inert solute. The BL two-dimensional orientational model presents a density anomaly and two liquid phases with different structures.[1]

We have presented a thorough investigation of two fixed concentrations of solute, respectively, 2% and 10%. Real gas presents somewhat smaller concentrations [36]. However, an exploratory study shows that the features examined by us are preserved as concentration is lowered down to realistic values. This justifies carrying out extensive simulations at the less realistic concentrations of 2% and 10%, since investigation of smaller concentrations requires much larger simulation boxes.

For both concentrations, but more evidently for 10% solute, the presence of solute "strengthens" the hydrogen bonds. Inspection and comparison of phase diagrams show that the structured phase is stabilized to higher temperatures, at fixed chemical potential, and to much higher chemical potentials. For the higher concentration of solute, the transition between the structured and the unstructured phases as chemical potential is varied disappears. Examination of solvent structure shows that the presence of solute nucleates patches of hydrogen-bonded solvent particles. Solute intercalates with properly oriented solvent. Both features, increments of water structure and solvent-separated solute states, have been reported from experiments and atomistic models [37].

Solubility of our small concentration of inert solute presents a minimum (TmS), which coincides with the maximum solvent density (TMD), as expected [28]. For interacting solute, a simple argument leads us to expect TmS to occur at higher temperatures for the BL solvent model.

Investigation of the latter point, as well as the effect of solute size, is the subject of ongoing work.

ACKNOWLEDGMENTS

We thank the Brazilian science agencies CNPq and Capes for financial support. This work is partially supported by CNPq, INCT-FCx.

[1] A modified form of the BL model has been investigated as to solvation entropy and enthalpy properties [35].

[1] T. L. Hill, *Statistical Thermodynamics* (Addison-Wesley, New York, 1960).
[2] R. Battino and H. L. Clever, Chem. Rev. **66**, 395 (1966).
[3] J. D. Bernal and R. H. Fowler, J. Chem. Phys. **1**, 515 (1913).
[4] T. Head-Gordon and G. Hura, Chem. Rev. **102**, 2651 (2002).
[5] C. L. Perrin and J. B. Nielson, Annu. Rev. Chem. **48**, 511 (1997).
[6] N. A. M. Besseling and J. Lyklema, J. Phys. Chem. **98**, 11610 (1994).
[7] G. M. Bell and D. A. Lavis, J. Phys. A **3**, 568 (1970).
[8] S. Sastry, P. G. Debenedetti, F. Sciortino, and H. E. Stanley, Phys. Rev. E **53**, 6144 (1996).
[9] C. J. Roberts and P. G. Debenedetti, J. Chem. Phys. **105**, 658 (1996).
[10] G. Franzese and H. E. Stanley, J. Phys.: Condens. Matter **14**, 2201 (2002).
[11] M. Pretti and C. Buzano, J. Chem. Phys. **121**, 11856 (2004).
[12] E. Lomba, N. G. Almarza, C. Martin, and C. McBride, J. Chem. Phys. **126**, 244510 (2007).
[13] N. G. Almarza, J. A. Capitan, J. A. Cuesta, and E. Lomba, J. Chem. Phys. **131**, 124506 (2009).
[14] P. C. Hemmer and G. Stell, Phys. Rev. Lett. **24**, 1284 (1970).
[15] E. A. Jagla, Phys. Rev. E **58**, 1478 (1998).
[16] M. C. Wilding and P. F. McMillan, J. Non-Cryst. Solids **293**, 357 (2001).
[17] P. J. Camp, Phys. Rev. E **68**, 061506 (2003).

[18] V. N. Ryzhov and S. M. Stishov, Phys. Rev. E **67**, 010201 (2003).
[19] D. Y. Fomin *et al*., J. Chem. Phys. **129**, 064512 (2008).
[20] G. Franzese, G. Malescio, A. Skibinsky, S. V. Buldyrev, and H. E. Stanley, Nature (London) **409**, 692 (2001).
[21] A. B. de Oliveira, P. A. Netz, T. Colla, and M. C. Barbosa, J. Chem. Phys. **124**, 084505 (2006).
[22] N. Barraz, Jr., E. Salcedo, and M. Barbosa, J. Chem. Phys. **131**, 094504 (2009).
[23] A. B. de Oliveira *et al*., J. Chem. Phys. **132**, 164505 (2010).
[24] V. B. Henriques and M. C. Barbosa, Phys. Rev. E **71**, 031504 (2005).
[25] C. E. Fiore, M. M. Szortyka, M. C. Barbosa, and V. B. Henriques, J. Chem. Phys. **131**, 164506 (2009).
[26] M. M. Szortyka, M. Girardi, V. B. Henriques, and M. C. Barbosa, J. Chem. Phys. **132**, 134904 (2010).
[27] M. M. Szortyka, C. E. Fiore, V. B. Henriques, and M. C. Barbosa, J. Chem. Phys. **133**, 104904 (2010).
[28] L. R. Pratt and D. Chandler, J. Chem. Phys. **67**, 3683 (1977).
[29] B. J. Berne, Proc. Natl. Acad. Sci. USA **93**, 8800 (1996).
[30] G. G. Hummer, S. Garde, A. E. García, A. Pohorille, and L. R. Pratt, Proc. Natl. Acad. Sci. USA **93**, 8951 (1996).
[31] B. Guilot and Y. Guissani, J. Chem. Phys. **99**, 8075 (1993).
[32] M. A. A. Barbosa and V. B. Henriques, Phys. Rev. E **77**, 051204 (2008).
[33] F. S. Bates, Science **251**, 898 (1991).
[34] B. Widom, J. Phys. Chem. **39**, 11 (1963).
[35] C. Buzano, E. B. De Stefanis, and M. Pretti, Phys. Rev. E **71**, 051502 (2005).
[36] National Institute of Standards and Technology, Standard Reference Database, http://webbook.nist.gov/chemistry, 2006.
[37] B. M. Laadanyi and M. S. Skaf, Annu. Rev. Phys. Chem. **44**, 3335 (1993).